

Wind Loading Standard for Building Design in Thailand and Country Report 2010

Virote Boonyapinyo^a, Nakhorn Poovarodom^a
Naret Limsamphancharoen^b, Nikhom Saterngram^c

^a Associate Professor, Department of Civil Engineering, Thammasat University
Rangsit Campus, Pathumthani 12120, Thailand

^b Assistant Professor, Department of Civil Engineering, Thammasat University
Rangsit Campus, Pathumthani 12120, Thailand

^c Civil Engineer, Department of Public Works and Town & Country Planning
Ministry of Interior

ABSTRACT: The new development of DPT Standard 1311-50 for wind loading calculation and response of buildings in Thailand is financially supported by Department of Public Works and Town & Country Planning. The new standard is more accurate than the building code No.6 because it considers the wind speed zoning, surrounding terrain, building shapes, and dynamic properties. The new standard format is widely used in the international codes. The new standard consists of 3 parts, namely, 1. Wind loading standard for building design, 2. Commentaries to the standard and 3. Numerical examples. Three different approaches for determining design wind loads on buildings are given in the standard, namely, the simple procedure for low- and mid-rise buildings, the detailed procedure for high-rise buildings, and wind-tunnel test procedure. Finally, examples of wind load studies of buildings and bridges by TU-AIT wind tunnel test are also presented.

KEYWORDS: Wind Loading Standard, DPT standard 1311-50, Thailand, Wind Tunnel Test, High-Rise Buildings, Long-Span Bridges

1. INTRODUCTION

The wind load specified in the existing building code under the Building Control Act (BCA) 1979 is obsolete because it does not consider the terrain conditions and the typhoon influence and then the wind pressures depend on only the height and apply the same value for whole country. In addition, the code value is too low for very tall building, and for building in open exposure, as well as buildings in the Southern part of Thailand which is prone to typhoon attack [1, 2]. Therefore, the subcommittee on wind and earthquake effects on structures of the Engineering Institute of Thailand published the wind loading standard for building design in 2003 [3]. It considers the wind speed zoning, surrounding terrain, dynamic properties, and building shapes. The standard is mainly based on the National Building Code of Canada 1995 [4].

However, the wind loading standard for building design in 2003 has been revised again for up-to-date wind loading standard. At present, DPT standard 1311-50 (Figure 1) for wind loading calculation and response of buildings in Thailand is newly published by Department of Public Works and Town & Country Planning [5]. To develop the new wind loading standard for building design, an evaluation and comparison of wind load and responses for building among several codes/standards were studied by Boonyapinyo et al. [5-

7], among others. The comparisons include National Building Code of Canada [8], International Standard [9], ASCE Standard [10], AIJ Recommendation [11], Australian Standard [12] and European Standard [13]. The new development of DPT standard 1311-50 for wind loading calculation and response of buildings over 2003 version includes the specified wind load and response, reference wind speed map, natural frequency and damping of building, table for design wind loads for main structures, secondary members and claddings for low-rise buildings, wind tunnel test procedure, commentary, numerical examples, computer program for calculation of wind load and response, and wind load on miscellaneous structures such as, large billboards, cylinders, poles, structural member, two- and three-dimensional trusses. The reference wind speed is based on the study of the wind climate in Thailand [1, 5, 14-15]. The wind speed for the Southern Thailand reflects the influence of the rare event of the typhoons in the region. The natural frequency and damping for building in Thailand are based on the measurements of 50 buildings in Bangkok [16].

2. WIND LOADING CALCULATION PROCEDURE

Three different approaches for determining design wind loads on buildings and structures are given in the standard as follows.

2.1 *Simple procedure*

The simple procedure is appropriate for use with the majority of wind loading applications, including the structure and cladding of low and medium rise building and the cladding design of high rise buildings. These are situations where the structure is relatively rigid. Thus, dynamic actions of the wind do not require detailed knowledge of the dynamic properties of the buildings and can be dealt with by equivalent static loads.



Figure 1. DPT standard 1311-50



Figure 2. Example of model in boundary-layer long-wind tunnel of TU-AIT.

2.2 *Detailed procedure*

The detailed procedure is appropriated for buildings whose height is greater than 4 times their minimum effective width or greater than 80 m and other buildings whose light weight, low frequency and low damping properties make them susceptible to vibration

2.3 Wind tunnel test procedure

Wind tunnel testing is appropriate when more exact definition of dynamic response is needed and for determining exterior pressure coefficients for cladding design on buildings whose geometry deviates markedly from more common shapes for which information is already available. Detail of wind tunnel test procedure is given in [5].

Figure 2 shows the boundary-layer long-wind tunnel that was jointly built by Thammasat University (TU) and Asian Institute of Technology (AIT) at Thammasat University. The test section is 2.5x2.5 m with 25.5 m in length. Wind speed is in the range of 0.5 to 20 m/s.

3. SPECIFIED WIND LOADING

The specified external pressure or suction due to wind on part or all of a surface of a building shall be calculated from

$$p = I_w q C_e C_g C_p \quad (1)$$

where

p = the specified external pressure acting statically and in a direction normal to the surface either as a pressure directed to wards the surface or as a suction directed away from the surface,

I_w = importance factor for wind load, as provided in Table 1,

q = the reference velocity pressure,

C_e = the exposure factor,

C_g = the gust effect factor,

C_p = the external pressure coefficient, averaged over the area of the surface considered

Table 1. Importance factor

Importance Category	Importance factor, I_w	
	Ultimate limit states	Serviceability limit states
Low	0.8	0.75
Normal	1	0.75
High	1.15	0.75
Post-disaster	1.15	0.75

The net wind load for the building as a whole shall be the algebraic difference of the loads on the windward and the leeward surfaces, and in some cases may be calculated as the sum of the products of the external pressures or suction and the areas of the surfaces over which they are averaged

The net specified pressure due to wind on part or all of a surface of a building shall be the algebraic difference of the external pressure or suction as given in Equation (1) and the specified internal pressure or suction due to wind calculated from

$$p_i = I_w q C_e C_g C_{pi} \quad (2)$$

where

- p_i = the specified internal pressure, acting statically and in a direction normal to the surface either as a pressure (directed outwards) or as a suction (directed inwards),
- q = the reference velocity pressure,
- C_e = the exposure factor, evaluated at the building mid-height instead of the height of the element considered,
- C_g = the gust effect factor,
- C_{pi} = the internal pressure coefficient

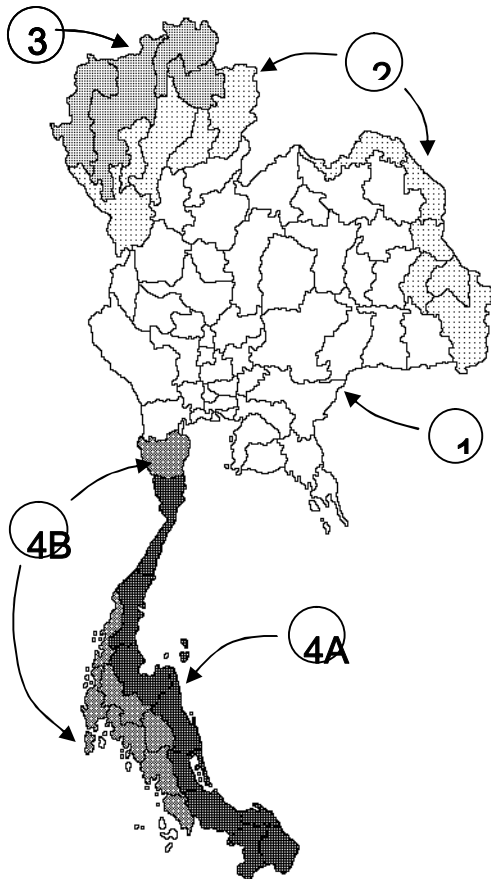


Figure 3. Reference wind speed zone for Thailand.

4. REFERENCE VELOCITY PRESSURE

The reference wind pressure, q , is determined from reference (or design) wind speed, \bar{V} by the following equation:

$$q(\text{in kg/m}^2) = \frac{1}{2} \left(\frac{\rho}{g} \right) \bar{V}^2 \quad (3)$$

where

- ρ = air density = 1.25 kg/m³
- g = acceleration due to gravity = 9.81 m/s²
- \bar{V} = design wind speed

$\bar{V} = V_{50}$ for serviceability limit state

$\bar{V} = T_F \cdot V_{50}$ for ultimate (strength) limit state

V_{50} = reference wind speed that is based on one-hour average wind speed at 10 m. in open terrain in 50-years return period. V_{50} and typhoon factor (T_F) are shown in Table 2 and Figure 3.

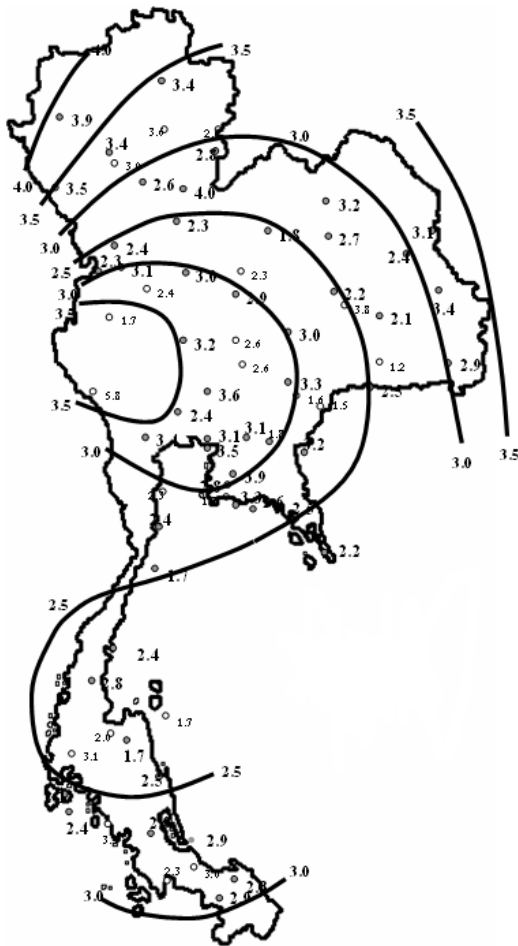


Figure 4. Contour of dispersion (or scale) factor [5, 15]

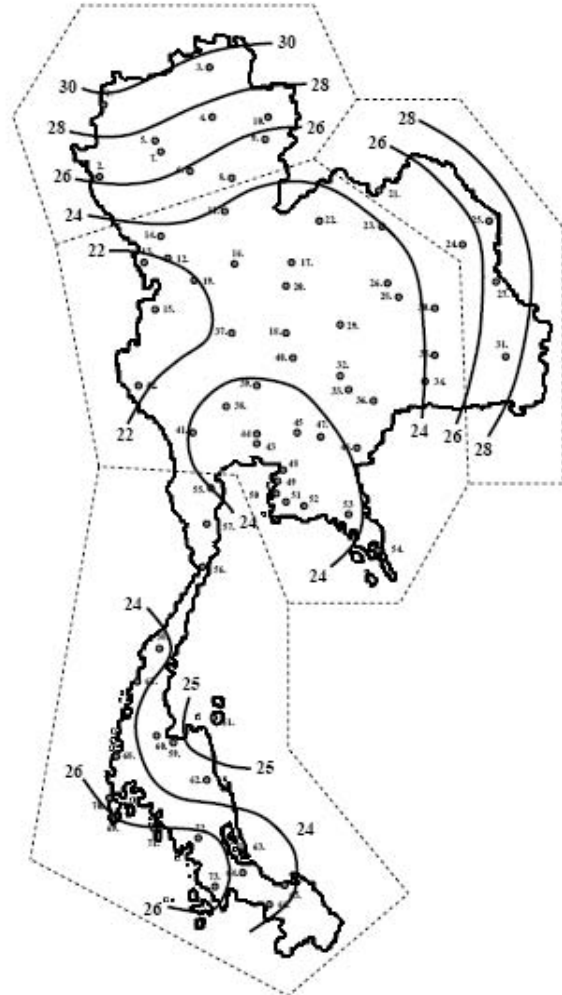


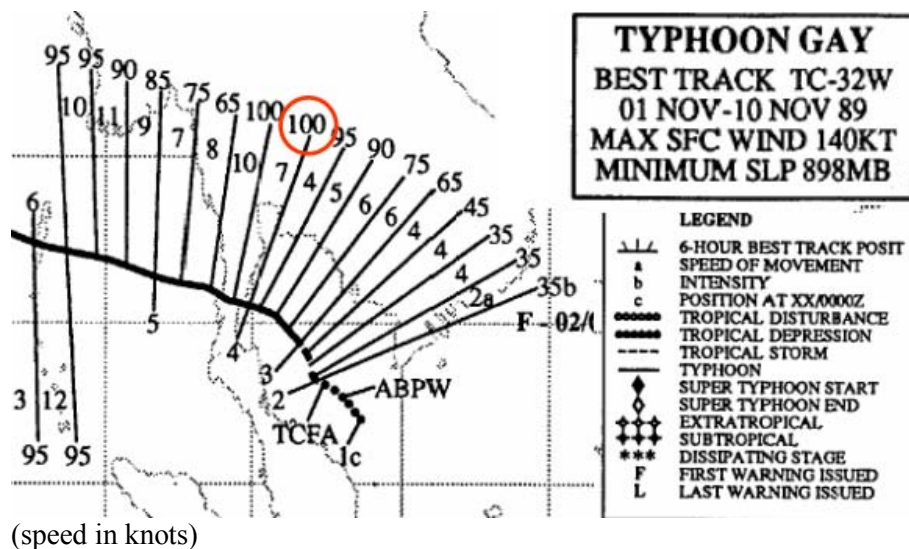
Figure 5. Location of 73 wind stations and contour of reference wind speed for 50-year return periods [5, 15]

In this study, the annual maximum wind speeds from 73 stations as shown in Figure 5 were used in extreme wind analysis [5, 15]. The data were converted to one-hour average speed at 10 m. in open terrain according to anemometer height and terrain of each station, and were fitted to a Type I extreme-value distribution using probability weighted moment method. Figures 4 and 5 show contour of dispersion (or scale) factor and referent wind speed for 50-year return periods, respectively [5, 15]. The analysis of dispersion map and the 50-years return period speeds indicate that the area can be divided in to four zones as shown in Figure 3. The 50-year return period speed for each zone was then estimated by the representative values of dispersion and location parameters of that zone. The higher wind speeds for Zone 2

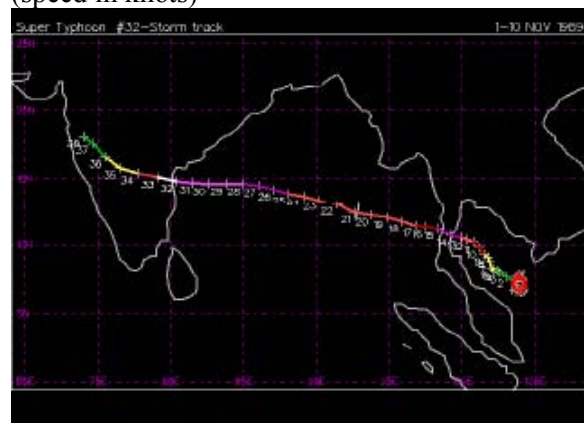
and 3 are due to the mixed effect of the weakening tropical storm entering the region from the east and the severe thunder storm happening in summer (from March to May) of every year.

Table 2. Reference wind speeds and typhoon factor

Zone	Area	V_{50}	T_F
Zone 1	Central region	25	1.0
Zone 2	Lower part of Northern region and East west border region	27	1.0
Zone 3	Upper part of Northern region	29	1.0
Zone 4 A	East coast of Southern peninsula	25	1.2
Zone 4 B	Petchaburi and West coast of Southern peninsula	25	1.08



(speed in knots)



Type	Category	Pressure (mb)	Winds (knots)	Winds (mph)	Surge (ft)	Line Color
Depression	TD	---	< 34	< 39		Green
Tropical Storm	TS	---	34-63	39-73		Yellow
Typhoon	1	> 980	64-82	74-95	4-5	Red
Typhoon	2	965-980	83-95	96-110	6-8	Light Red
Typhoon	3	945-965	96-112	111-130	9-12	Magenta
Typhoon	4	920-945	113-135	131-155	13-18	Light Magenta
Super Typhoon	5	< 920	>135	>155	>18	White

Figure 6. Typhoon Gay track [17]

The design wind speed of Zone 4 is governed by the South-west and the North-east Monsoons which give a design wind speed as low as 25 m/s. However, the historical records indicate that tropical cyclone may affect this region especially in November and December. In 1989, Typhoon Gay which developed in the Gulf of Thailand had crashed into Chumporn. It is reported that Typhoon Gay has a one-minute sustained surface wind speed of 100 knots (51.4 m/s.) as shown in Figure 6 [17], which corresponding to a one-hour average speed of 41.1 m/s. At least 600 people were killed, and more than 46,000 houses were either totally or partially destroyed by this typhoon. The design wind speed of this zone must take into account the effect of tropical cyclone to ensure that the post-disaster buildings must not

collapse if a typhoon with the same intensification as Typhoon Gay would happen again. As a result, it is considered that the post-disaster buildings in this zone must be able to sustain the wind pressure developed by a wind speed of 41.1 m/s. at ultimate state. With the load factor of 1.6 and importance factor for post-disaster of 1.15, the corresponding design wind speed for zone 4 is thus $41.1/\sqrt{1.6*1.15} = 30.3 \approx 30$ m/s. Therefore, the typhoon factor for east coast of southern peninsula = $30/25 = 1.2$. However, the typhoon factor in Table 2 should be applied for buildings and structures that have importance category as post-disaster. For others, it is subjected to designer judgment.

5. EXPOSURE FACTOR

The exposure factor, C_e , reflects changes in wind speed and height, and also the effects of variations in the surrounding terrain and topography. The exposure factors for use with either the simple or detailed procedure are given as follows.

5.1 Simple procedure

Exposure A: (open or standard exposure): open level terrain with only scattered buildings, trees or other obstructions, open water or shorelines thereof.

$$C_e = \left(\frac{Z}{10}\right)^{0.2}, \quad C_e \geq 0.9 \quad (4)$$

Exposure B: suburban and urban areas, wooded terrain or center of large towns.

$$C_e = 0.7\left(\frac{Z}{12}\right)^{0.30}, \quad C_e \geq 0.7 \quad (5)$$

In Equations (4) to (5), Z is the height above ground in metre.

5.2 Detailed procedure

For the detailed procedure, the exposure factor, C_e , is based on the mean wind speed profile, which varies considerable depending on the general roughness of the terrain over which the wind has been blowing before it reaches the building. To determine the exposure factor, three categories have been established as follows:

Exposure A: (open or standard exposure): open level terrain with only scattered buildings, trees or other obstructions, open water or shorelines thereof. This is the exposure on which the reference wind speeds are based.

$$C_e = \left(\frac{Z}{10}\right)^{0.28} \quad \text{for } 1.0 \leq C_e \leq 2.5 \quad (6)$$

Exposure B: suburban and urban areas, wooded terrain or center of large towns.

$$C_e = 0.5\left(\frac{Z}{12.7}\right)^{0.50} \quad \text{for } 0.5 \leq C_e \leq 2.5 \quad (7)$$

Exposure C: center of large cities with heavy concentrations of tall buildings. At least 50% of the buildings should exceed 4 stories. This exposure is only applicable to the heavily built-up center of large cities and should be used with caution because of local channeling and wake buffeting effects that can occur near tall buildings.

$$C_e = 0.4 \left(\frac{Z}{30} \right)^{0.72} \text{ for } 0.4 \leq C_e \leq 2.5 \quad (8)$$

In Equations (6) to (8), Z is the height above ground in metre.

Exposure B or C should not be used unless the appropriate terrain roughness persists in the upwind direction for at least 1 km or 10 times the height of the building, whichever is larger, and the exposure factor should be recalculated if the roughness of terrain differs from one direction to another.

6 GUST EFFECT FACTOR

The gust effect factor, C_g , is defined as the ratio of the maximum effect of the loading to the mean effect of the loading. The dynamic response includes the action of

- a) random wind gusts action for short durations over all or part of the structure.
- b) fluctuating pressures induced by the wake of the structure, including “vortex shedding forces,” and
- c) fluctuating forces induced by the motion of the structure itself through the wind.

The gust effect factor for use with either the simple or detailed procedure are given as follows.

6.1 Simple procedure

The gust effect factor C_g is one of the following values:

- a) 2.0 for the building as a whole and main structural member,
- b) 2.5 for external pressures and suctions on small elements including cladding
- c) 2.0 or a value determined by detailed calculation for internal pressures (see standard [5])

6.2 Detailed procedure

The gust effect factor is calculated as

$$C_g = 1 + g_p (\sigma / \mu) \quad (9)$$

where

- μ = the mean loading effect,
- σ = the “root-mean square” loading effect, and
- g_p = a statistical peak factor for the loading effect obtained from figure in the standard.

The value of σ / μ can be expressed as

$$\sigma / \mu = \sqrt{\frac{K}{C_{eH}} \left(B + \frac{sF}{\beta} \right)} \quad (10)$$

where

K	= a factor related to the surface roughness coefficient of the terrain, = 0.08 for Exposure A , = 0.10 for Exposure B , = 0.14 for Exposure C ,
C_{eH}	= exposure factor at the top of the building, H ,
B	= background turbulence factor obtained from figure in the standard as a function of W/H ,
W	= width of windward face of the building,
H	= height of windward face of the building,
s	= size reduction factor obtained from figure in the standard as a function of W/H and the reduced frequency $n_o H/V_H$,
n_o	= natural frequency of vibration, Hz . Values recommended in the design of concrete building = $44/H$ [5, 16],
V_H	= mean wind speed (m/s) at the top of structure, H ,
F	= gust energy ratio at the natural frequency of the structure obtained from Figure in the standard as a function of the wave number, n_o/V_H , and
β	= damping ratio. Suggested values for β must be based mainly on experiments on real structures. Values commonly used in the design of building with steel frames and concrete frames are in the range of 0.005 and 0.015 [5, 16].

7 PRESSURE COEFFICIENTS

Pressure coefficients are the non-dimensional ratios of wind-induced pressures on a building to the dynamic pressure (velocity pressure) of the wind speed at the reference height. Pressures on the surfaces of structures vary considerably with the shape. Wind direction and profile of the wind velocity.

The information on external and internal pressure coefficients given in the standard covers requirements for the design of the cladding and the structure as a whole for a variety of simple building geometries.

For rectangular shape building, the external pressure coefficients for windward and leeward walls are 0.8 and -0.5 , respectively, as shown in Figure 7. Reference heights for exposure factor for the calculation of both spatially-averaged and local pressures are as follows. Leeward walls use at $0.5 H$, roof and side walls use at H , any area at height Z above ground on the windward wall use at Z .

A local pressure coefficient, $C_p^* = \pm 0.9$, applicable to the design of small cladding areas (about the size of a window), can occur almost anywhere at any elevation. However, the local $C_p^* = -1.2$ given for corners apply to an edge zone of $0.1D$ wide.

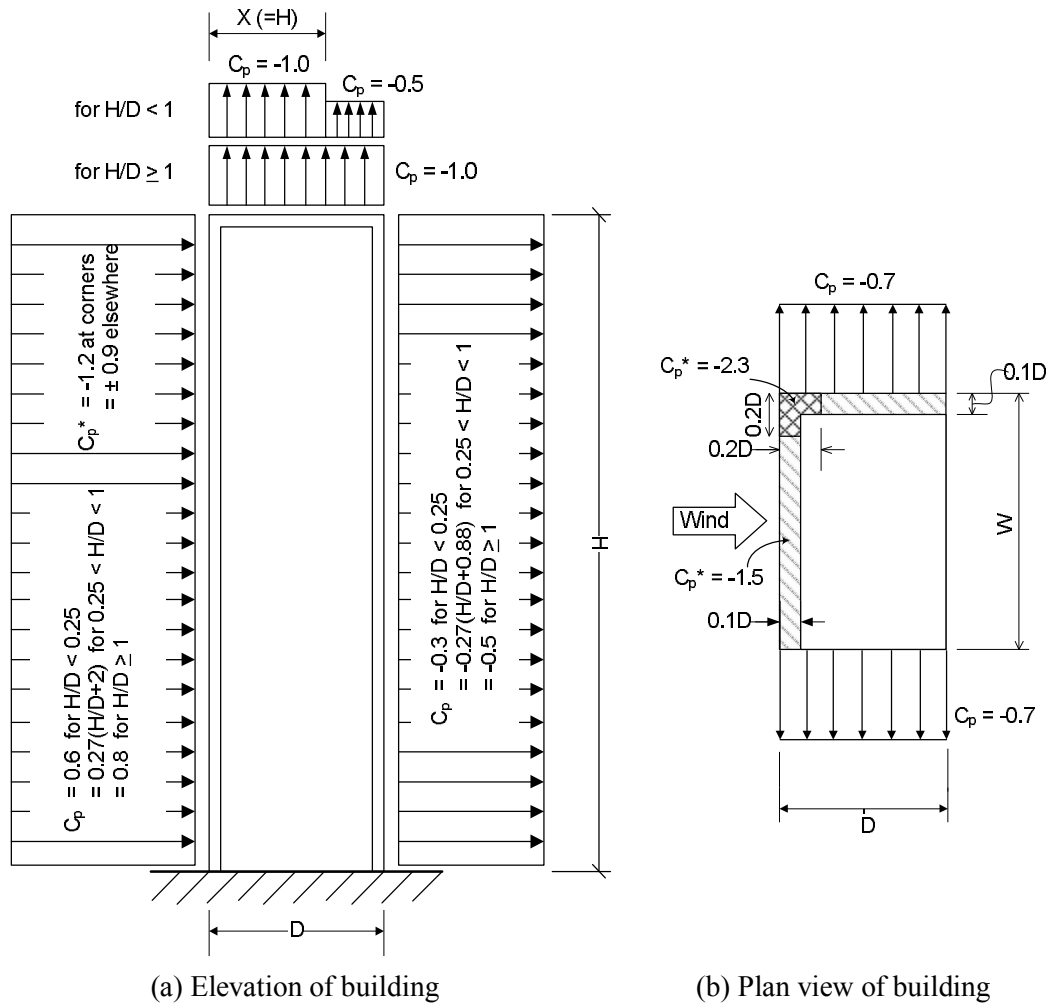


Figure 7. External pressure coefficients, C_p and C_p^* , for flat-roofed buildings greater in height than in width

8. LATERAL DEFLECTION

Lateral deflection of tall buildings under wind loading may require consideration from the standpoints of serviceability or comfort. A maximum lateral deflection limitation of $1/500$ of the building height with importance factor of 0.75 for serviceability limit states is specified.

9. BUILDING MOTION

While the maximum lateral wind-loading and deflection are generally in the direction parallel with the wind (along-wind direction), the maximum acceleration of a building leading to possible human perception of motion or even discomfort may occur in the direction perpendicular to the wind (across-wind direction) if \sqrt{WD}/H is less than one-third, where W and D are the across-wind and along-wind building dimensions and H is the height of the building.

The maximum acceleration in the along-wind direction can be found from the expression

$$a_D = 4\pi^2 n_D^2 g_p \sqrt{\frac{KsF}{C_{eH}\beta}} \cdot \frac{\Delta}{C_g} \quad (11)$$

where

- a_D = peak acceleration in along wind direction, m/s^2 ,
- ρ_b = average density of the building, kg/m^3 ,
- β = damping ratio in along-wind direction,
- n_D = fundamental natural frequencies in along-wind direction, Hz .
- Δ = maximum wind-induced lateral deflection at the top of the building in along-wind direction, m.

An acceleration limitation of 1.5 to 2 % of gravity is specified for use in conjunction with Equation (11) and in the across-wind direction with importance factor of 0.75 for serviceability limit states. The lower value is considered appropriate for apartment buildings, the higher value for office buildings.

10. ACROSS-WIND AND TORSIONAL LOAD AND RESPONSE

Across-wind and torsional load and response in DPT standard 1311-50 are based on the AIJ Recommendation [18]. Details are given in Reference 5.

11. EXAMPLES OF WIND LOAD STUDY BY TU-AIT WIND TUNNEL TEST

11.1 *Wind load study for cladding design*

a. *MahaNakhon Building in Bangkok*

Wind load study for cladding design of MahaNakhon Building was performed by TU-AIT wind tunnel test as shown in Figures 2 and 8 [19]. The MahaNakhon Building is located in the embassy/financial district in the centre of Bangkok between the Sathon and Silom roads. The area surrounding the studied building generally consists of urban development in all directions from the site. The studied building has 39 m square in plan, 309.9 m in roof height, and has surface “pixellations”. The studied building was specially constructed by an acrylic rigid model. The 1:400 scale models of studied building and its surrounding buildings within 400 m radius from the studied building were mounted on a 2-m diameter turntable, allowing any wind direction to be simulated by rotating the model to the appropriate angle in the wind tunnel. The studied building model and its surroundings were tested in a boundary layer wind tunnel where the mean wind velocity profile, turbulence intensity profile, and turbulence spectrum density function of the winds approaching the study site are simulated for urban exposure based on the ASCE7 Standard [10] and ASCE Manual and Reports on Engineering Practice No. 67. In this study, overall wind load obtained from a wind tunnel test were measured on a direction-by-direction basis for 36 directions at 10-degree intervals, on the 1:400 scale model of the building exposed to an approaching wind.

According to the DPT Standard 1311-50 [5], the reference velocity pressure, q , for the design of main structure and cladding shall be based on a probability of being exceeded in any one year of 1 in 50 (50-year return period) corresponding to reference wind speed of 25 m/s at the height of 10 m in open terrain. Because the proposed building is located in the Central Bangkok with heavy concentrations of tall buildings, the exposure C (center of large cities) was applied in this study, and the typhoon factor = 1.0. Then design wind speed is 25

m/s, and corresponding to design wind speed of 36.65 m/s at the 309.9 m roof height in the exposure C.

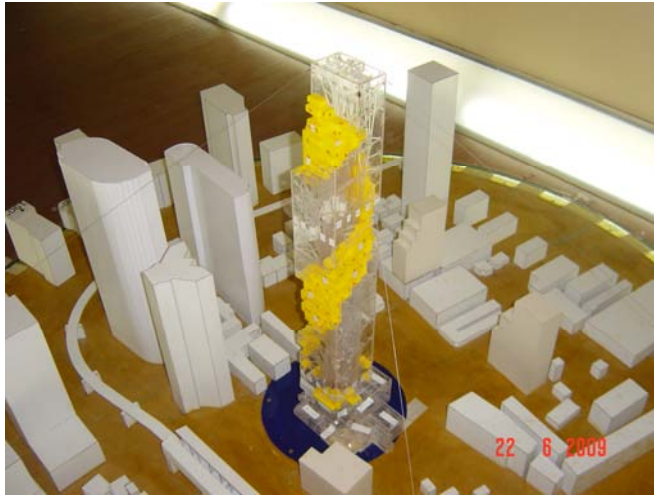


Figure 8. Rigid model of MahaNakhon building in Bangkok

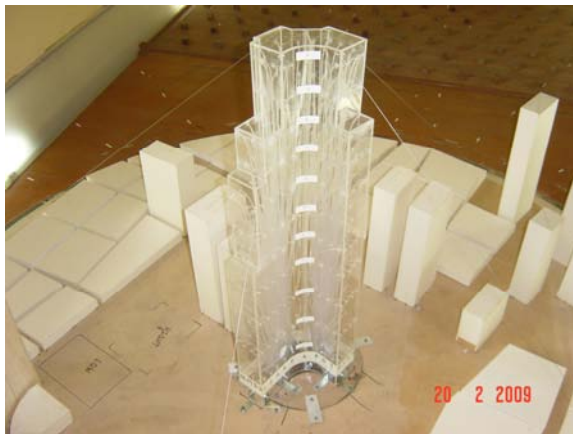


Figure 9. Rigid model of Gramercy building in Manila



Figure 10. Rigid model of Knightbridge building in Manila

b. Gramercy building and Knighrbridge building

In addition, wind load studies for cladding design of Gramercy building and Knighrbridge building in Manila were performed by TU-AIT wind tunnel test as shown in Figures 9 and 10 [20].

11.2 Wind load study for overall fluctuating loads and dynamic response

a. MahaNakhon Building in Bangkok

Wind load study for overall fluctuating loads and dynamic response of MahaNakhon Building was performed by TU-AIT wind tunnel test as shown in Figure 11 [19]. The studied building has 39 m square in plan, 309.9 m in roof height, and has surface “pixellations”. The studied building was specially constructed by a light-weight rigid model,

such as balsa wood model, and the studied model was mounted on a high-frequency base balance. The 1:400 scale models of studied building and its surrounding buildings within 400 m radius from the studied building were mounted on a 2-m diameter turntable, allowing any wind direction to be simulated by rotating the model to the appropriate angle in the wind tunnel. The studied building model and its surroundings were tested in a boundary layer wind tunnel where the mean wind velocity profile, turbulence intensity profile, and turbulence spectrum density function of the winds approaching the study site are simulated. In this study, overall wind load obtained from a wind tunnel test were measured on a direction-by-direction basis for 36 directions at 10-degree intervals, on the 1:400 scale model of the building exposed to an approaching wind.

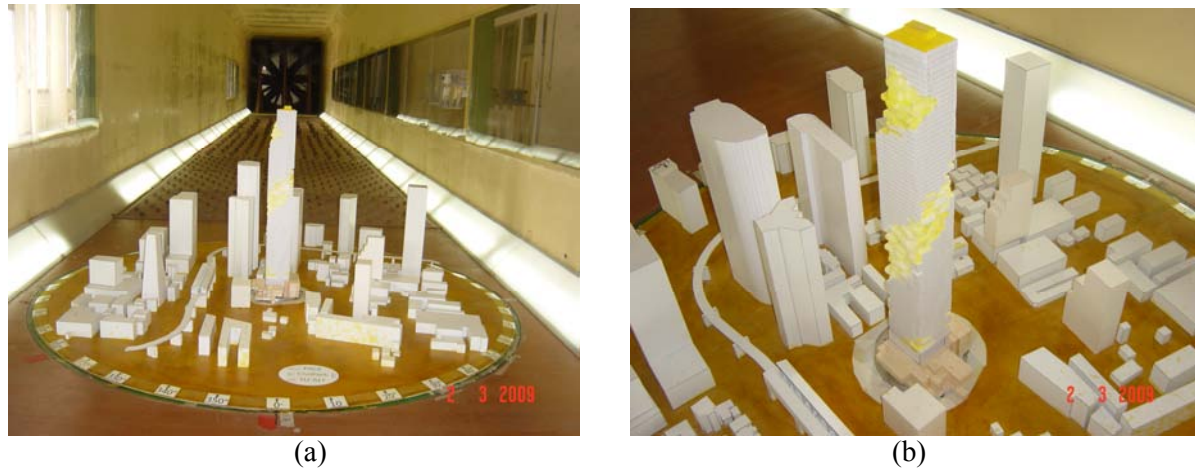


Figure 11. (a) Overall wind load study of MahaNakhon building in Bangkok by wind tunnel test, and (b) high-frequency force balance model

According to the DPT Standard 1311-50 [5], the reference velocity pressure, q , for the design of main structure and cladding shall be based on a probability of being exceeded in any one year of 1 in 50 (50-year return period) corresponding to reference wind speed of 25 m/s at the height of 10 m in open terrain. Because the proposed building is located in the Central Bangkok with heavy concentrations of tall buildings, the exposure C (center of large cities) was applied in this study, and the typhoon factor = 1.0. Then design wind speed is 25 m/s, and corresponding to design wind speed of 36.65 m/s at the 309.9 m roof height in the exposure C. For the serviceability design, the reference velocity pressure, q , shall be based on 10-year return period corresponding to reference wind speed of 20.25 m/s at the height of 10 m in open terrain. Therefore, corresponding design wind speed is 29.69 m/s at the 309.9 m roof height in the exposure C.

Table 3. Comparison of the expected peak base moments and torques for three values of natural frequencies f_o and two values of damping ratios ξ

Absolute Peak Base Moments or Torques (MN-m)	Damping ratio ξ = 0.01			Damping ratio ξ = 0.02		
	$0.8f_o$	f_o	$1.25f_o$	$0.8f_o$	f_o	$1.25f_o$
	My	9,223	5,601	3,701	6,580	4,047
Mx	7,066	4,508	3,278	5,051	3,271	2,852
Mz	82	77	72	71	68	64

For strength consideration with V_{50} (i.e. high return periods of wind velocity and high stress levels), three natural frequencies ($0.8 f_o$, f_o , and $1.25 f_o$) of studied building in each direction of motion, and two damping ratios ($\xi = 0.01$ and 0.02) are considered. Therefore, they are 6 cases of results. The results of expected peak base moments and torques for these six cases are shown and compared in Table 3. The results show that the peak base moments M_x and M_y are strongly dependent on both building natural frequencies and damping ratio. This is because both peak M_x and M_y are mainly caused by the acrosswind load, in which the acrosswind spectra exhibit an evident peak around the reduced frequency (Strouhal number) of 0.1.

For damping ratio $\xi = 0.02$ for strength consideration, the results found that the absolute peak base moments M_x of 3,271 MN-m, M_y of 4,047 MN-m and torque M_z of 68 MN-m occur at wind direction 0, 90, and 290 degree, respectively. The peak base moments M_x and M_y are strongly caused by the acrosswind load.

For serviceability consideration with V_5 and V_{10} (i.e. low return periods of wind velocity and low stress levels), three natural frequencies ($0.8 f_o$, f_o , and $1.25 f_o$) of studied building in each direction of motion, four damping ratios ($\xi = 0.005, 0.0075, 0.01, \text{ and } 0.03$ (with additional damping)), are considered. Therefore, they are 24 cases of results. The predicted peak acceleration responses for two values of return periods of V_5 and V_{10} , and four values of damping ratios ξ are shown and compared in the Figure 12 for natural frequencies f_o . The results show that the predicted peak acceleration responses are strongly dependent on the building natural frequencies, damping ratio, and return periods of wind velocity. This is because the peak acceleration responses are mainly caused by the acrosswind load, in which the acrosswind spectra exhibit an evident peak around the reduced frequency (Strouhal number) of 0.1.

According to the DPT Standard 1311-50 [5], the recommended serviceability design for human comfort criteria for the studied building is that the peak acceleration under a 10 year return period should be less than 15 mg and 25 mg for residential buildings and commercial buildings, respectively. For natural frequencies of building = $0.8 f_o$, f_o , and $1.25 f_o$, the predicted peak accelerations are found below the recommended criteria of 15 mg for the residential studied building when damping ratios are greater than about 0.015, 0.0075, and 0.005, respectively.

The ISO recommended serviceability design for human comfort criteria [21] depending on the building's lowest natural frequency is that the peak acceleration under a 5 year return period should not exceed $0.928 f^{-0.412}$ (in % of g) where f is the lowest natural frequency in Hz, and corresponding to 22 mg, 20 mg, and 18 mg when natural frequencies of studied building = $0.8 f_o$, f_o , and $1.25 f_o$, respectively. The predicted peak accelerations for three values of natural frequencies are found below the recommended criteria when damping ratio is greater than 0.005. The criteria of DPT Standard are more conservative than the ISO criteria especially for the residential studied building.

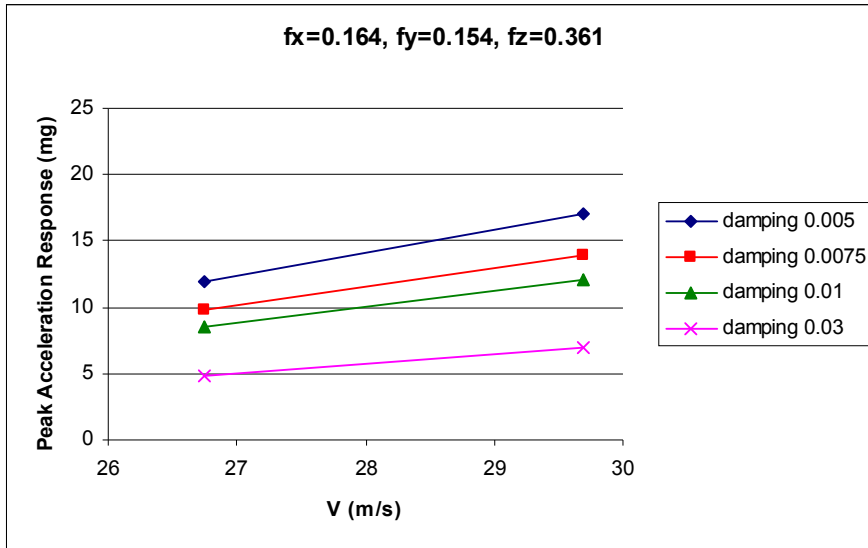


Figure 12. Comparison of predicted peak acceleration responses for two values of return periods of V_5 and V_{10} , and four values of damping ratios ξ (natural frequencies f_o)

b. Ramada Bangkok Sukhumvit Project

In addition, wind load studies for overall fluctuating loads and dynamic response of Ramada Bangkok Sukhumvit Project [22] were performed by TU-AIT wind tunnel test as shown in Figure 13.



Figure 13. (a) Overall wind load study of Ramada Bangkok Sukhumvit Project by wind tunnel test, and (b) high-frequency force balance model

11.3 *Wind load study for aerodynamic response of cable-supported bridges*

Flutter derivatives are the essential parameters in the estimations of the critical wind velocity for flutter-instability and the responses of long-span cable supported bridges. These derivatives can be experimentally estimated from wind tunnel tests results. Most of previous studies have used deterministic system identification techniques, in which buffeting forces and responses are considered as noises. In this research [23], the covariance-driven stochastic subspace identification technique (SSI-COV) was presented to extract the flutter derivatives of bridge decks from the buffeting test results. An advantage of this method is

that it considers the buffeting forces and responses as inputs rather than as noises. The Industrial Ring Road (IRR) cable-stayed bridge crossed Chao Phraya River with main span of 398 m (Figure 14) was applied for 1:90 scale sectional model test in TU-AIT wind tunnel test as the study case. Wind tunnel tests were performed for four section bridge models, i.e. original section (Figure 15), fairing-modified section, soffit plate modified section, and combination of those two modified section (Figure 16).



Figure 14. Three-dimensional view of IRR cable-stayed bridge



Figure 15. Original section of IRR bridge in wind tunnel



Figure 16. Fairings and soffit plates modified section in wind tunnel

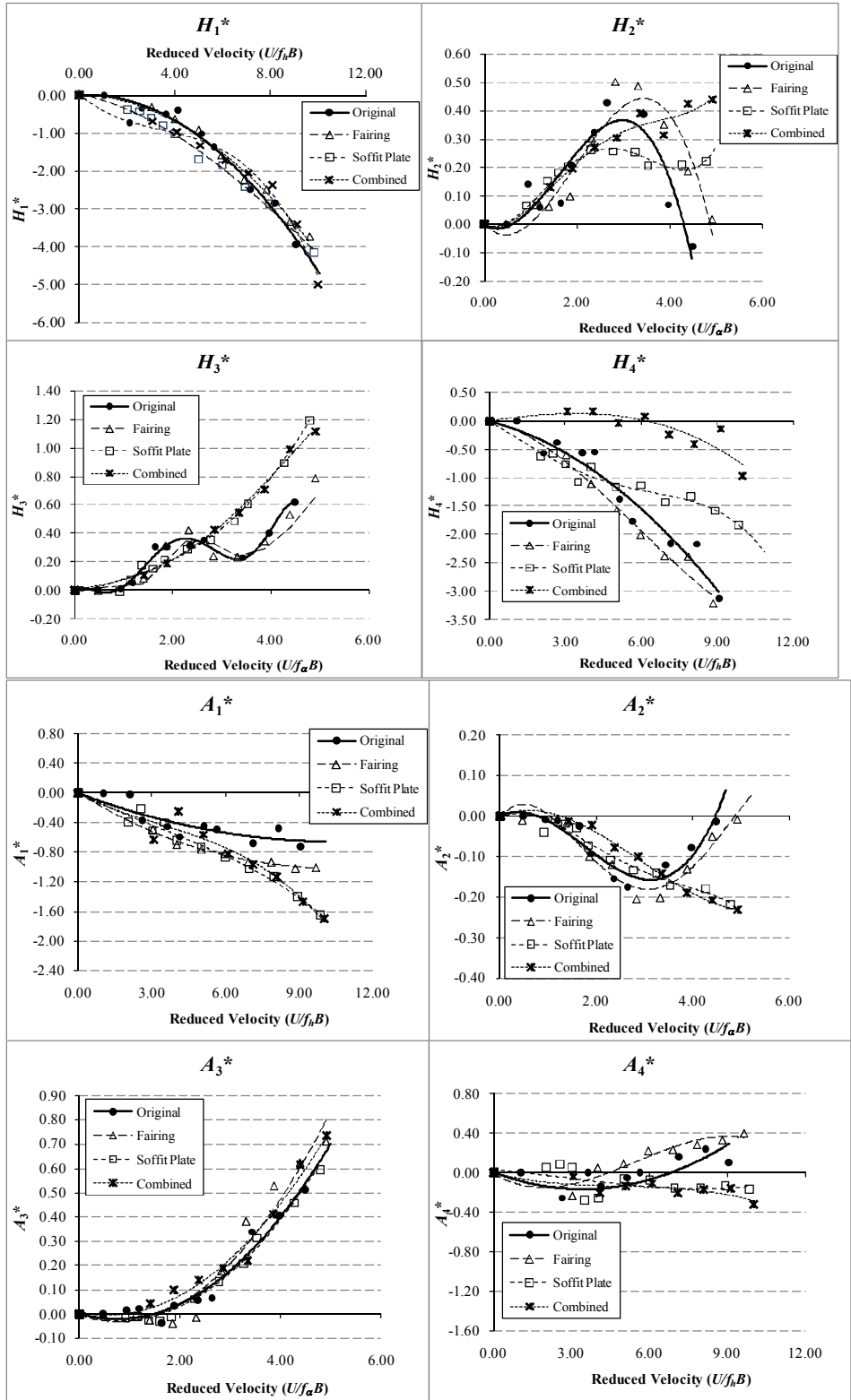


Figure 17. Comparisons of flutter derivatives among original section and modified sections [23]

a. Flutter derivatives [23]

The most important terms are H_1^* and A_2^* which refer respectively on vertical and torsional damping of the section. Their positive values indicate unstable conditions. For vertical aerodynamic damping coefficient, H_1^* , the modification effects considered to be negligible, which all sections show in negative region. However, the section are influenced by the

modifications in A_2^* which is most considerable in long-span bridges. The original section and fairing modified section lead to a single torsional flutter at high wind velocity because A_2^* change from negative values to positive values (Figure 17). Flutter derivatives H_2^* term, cross derivatives to a torsional aerodynamic damping, are conversely agree well with A_2^* results. Fairing modified section shows a little improvement on the unstable behavior, delaying the unstable of bridge deck from reduced velocity of 4.5 to 5. Also, it was clearly found that soffit plate modified section, and combination of soffit plate and fairings modified sections produce more stable sections, whereas the classical flutter rather than the single torsional flutter will occur because of H_2^* and A_1^* . Moreover, all modified sections show a little influence in A_1^* and A_3^* , which agree altogether well in trend. For H_3^* term, the fairings section agrees in trend with an original one, while soffit plates and combined sections are agree in trend to each other.

b. Structural responses and critical wind speeds [23]

Critical wind speed of original section was found at reduced wind velocity of 4.5 (Figure 18), corresponding to 118 m/s in full-scale (7.45 m/s in model scale). Flutter was found under single degree-of-freedom, torsional condition. On one hand, fairing-modified section can delay the critical wind speed up to velocity of 135 m/s in full scale or around 15% increased, compared with original section. On the other, for soffit plate modified section, and combination of soffit plate and fairings modified sections, flutter phenomenon was not found in testing velocity range.

The results found that the original section result in high vortex-shedding response and lead to a single torsional flutter at high wind velocity. The results also indicated that the combined fairing and soffit plate modified section is the most aerodynamic shape. When compared with the original section, this modified section can: a) suppress the vortex shedding significantly, b) result in the classical flutter rather than the single torsional flutter, and c) greatly increase the flutter velocity.

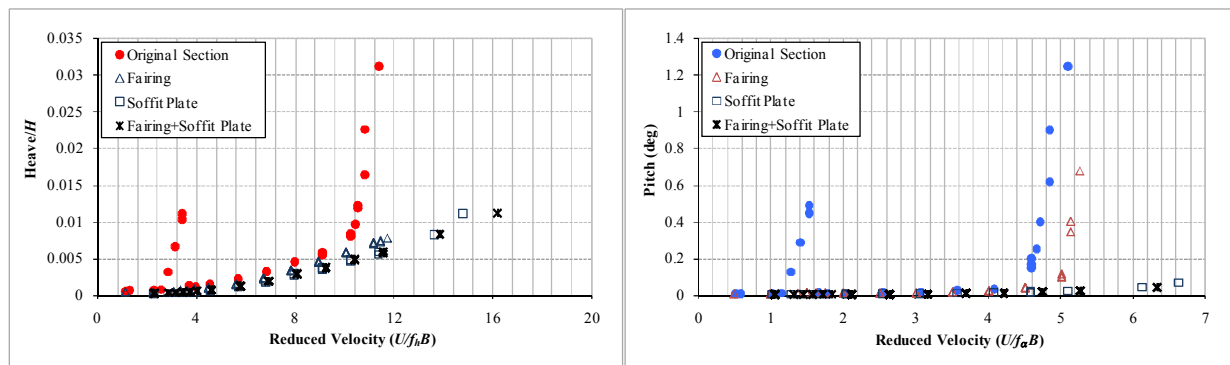


Figure 18. Comparisons of normalized heave and pitch responses among original section and three modified sections [23]

c. Effects of turbulent flow on flutter derivatives and responses of bridge deck [24]

In this research [24], the data-driven stochastic subspace identification technique (SSI-DATA) was presented to extract the flutter derivatives of bridge decks from the buffeting test results under smooth and turbulent flows (Figure 19). Most of the prototype bridges are exposed to turbulent wind; therefore, detailed investigations of the effects of turbulence on the flutter derivatives are significant. Almost all the wind tunnel tests for flutter derivatives have been generally carried out in smooth flows. Although few researchers have studied the problem using wind tunnel tests, in general, the results are still debatable and

inconclusive. For streamlined section, tests showed little effect [25], while tests on a rectangular box girder bridge showed galloping in smooth flow [26]. For Π type section, the effects of turbulence on the H_3^* and A_3^* seemed to be negligible [27]; whereas the other four derivatives related to aerodynamic damping characteristics showed some deviations from those in smooth flow, especially at high reduced wind speed.



Figure 19 IRR bridge model and grids to generate turbulent flow in wind tunnel

Figure 20 presents the identified flutter derivatives of the original IRR bridge deck by the SSI-DATA method from buffeting responses under smooth flow and two turbulent wind flows with both the longitudinal and the vertical turbulence intensities about 5% and 8%, respectively. Generally, the flutter derivatives of the bridge in turbulent flow identified by the SSI-DATA are in agreement with those in smooth flow. From Figure 20, it can be found that the influence of the flow type on H_4^* and A_3^* , i.e. flutter derivatives related to the direct aerodynamic stiffness, seems to be negligible. Though, the value of H_4^* obtained from the turbulent flow is somewhat less than that in the smooth flow case, it affected only the second decimal digit of the frequency value. The influence also has negligible effect on H_1^* and H_2^* i.e. direct and cross derivatives that are related to the vertical and the torsional aerodynamic damping, respectively. On the other hand, the remaining derivatives: A_1^* , A_2^* and H_3^* , show noticeable deviations from those in the smooth flow, especially at high wind speeds. The noticeable effect is that the reduced wind speed, which corresponds to the reversed sign of the torsional aerodynamic damping A_2^* , increased from 4.5 in the smooth flow to 5.1 in the 5% turbulent flow (Figure 20). It appears that for bluff type sections similar to the IRR Bridge, turbulence tends to make bridges more aerodynamically stable by delaying the torsional flutter. The deviations of flutter derivatives in this study may reveal that for those bridges with bluff type sections similar to the IRR Bridge, the effects of turbulence may be significant. Hence, both smooth and turbulent flow conditions are relevant; and the wind tunnel tests of such bridges for flutter derivative estimation should also be carried out in turbulent flows.

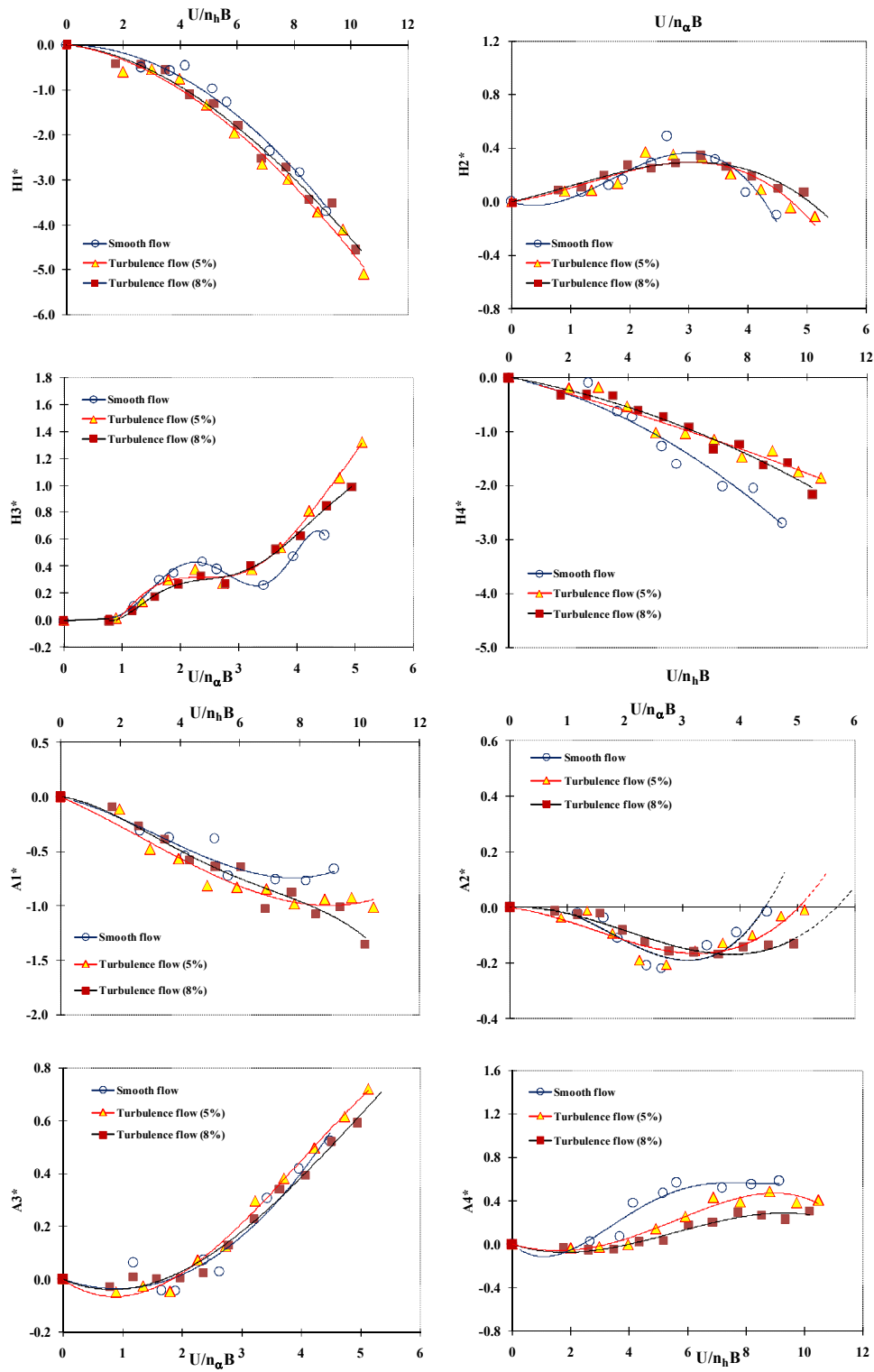


Figure 20 Flutter derivatives (A_i^*) of the original IRR Bridge model by SSI-DATA from buffeting responses under smooth and turbulent flows.

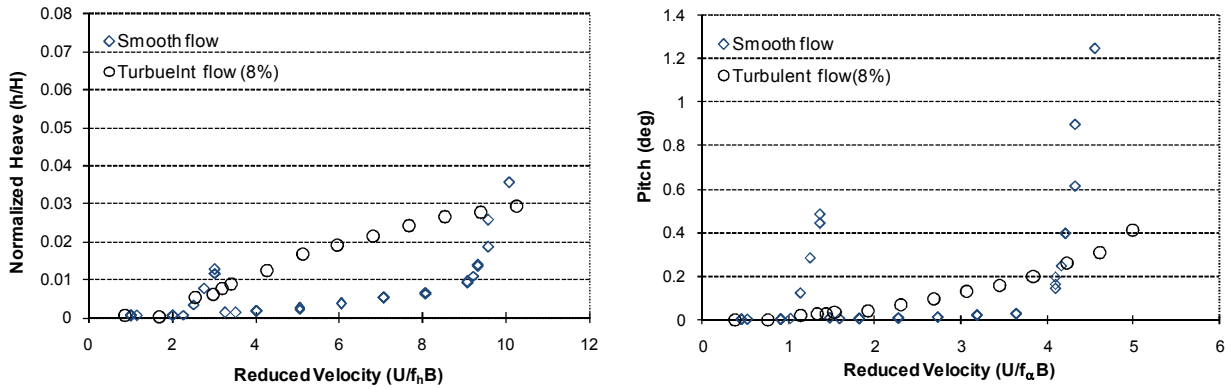


Figure.21 Vertical (Heave) and torsional RMS responses of the original IRR bridge model under smooth and turbulent flows.

Figure 21 shows comparisons of the root-mean-square (RMS) torsional and vertical buffeting responses of the IRR bridge model versus the reduced velocity between smooth and turbulent flow. Under a smooth flow, the very abrupt transition with increasing velocity from the effectively zero torsional response amplitude to the clear instability occurs in the near neighborhood of the reduced velocity value of 4.5 (Figures 20 and 21). The abrupt change in the vertical response at high wind speed is due to the effect of cross derivatives H_2^* and H_3^* which causes the coupling of the torsional responses with the vertical responses in terms of damping and stiffness, respectively [28]. Compared with the smooth flow, the turbulent flow reduces the vortex-shedding response; because, for the two-edge girder blunt type of IRR Bridge and similar sections, the turbulence tends to enhance the reattachment of flow and weaken the vortex shedding formulation. However, it raises the amplitude of the bridge responses progressively over the speed range. No clear and uniquely definable “flutter instability” was made evident in the range of wind velocity test.

12. CONCLUSIONS

The new development of DPT standard 1311-50 for wind loading calculation and response of buildings in Thailand is newly published by Department of Public Works and Town & Country Planning. Three different approaches for determining design wind loads on building are given in the standard, namely, the simple procedure for low-rise building, the detailed procedure for high-rise building, and wind-tunnel test procedure. The standard includes the calculation of: (1) wind load of the main wind resistant system and cladding; (2) lateral deflection; and (3) building motion in the along-wind and across-wind directions.

The new development of wind loading standard for building design in Thailand includes the specified wind load and response, reference wind speed map, natural frequency and damping of building, table for design wind loads for main structures, secondary members and claddings for low-rise buildings, wind tunnel test procedure, commentary, numerical examples, computer program for calculation of wind load and response, and wind load on miscellaneous structures such as, large billboards, cylinders, poles, structural member, two- and three-dimensional trusses.

Since the new development of DPT standard 1311-50, wind load standard and wind load studies of buildings and bridges by TU-AIT wind tunnel test have been increasingly interesting to Thai engineers.

13. ACKNOWLEDGEMENTS

The new development of wind loading standard for building design in Thailand is financially supported by Department of Public Works and Town & Country Planning. The first author is the project head. The author would like to thank the following persons for their supports in information for writing this paper: Assoc. Prof. Dr. Pennung Warnitchai of Asian Institute of Technology, and Prof. Dr. Panitan Lukkunaprasit of Chulalongkorn University.

14. REFERENCES

1. Lukkunaprasit, P., Pheinsusom, P., and Euasiriwam, N., (1995), Wind Loading for Tall Building Design in Thailand, Proc. of 2nd National Convention on Civil Engineering, Chiangmai, Thailand, pp. 51-61(in Thai).
2. Boonyapinyo, V., (1998), Comparison between Wind and Earthquake Loads for High-Rise Building Design in Thailand, Proc. of International Seminar on Earthquake Resistant Design of Structures, Chiangmai, Thailand., pp. 416-432 (in Thai).
3. Engineering Institute of Thailand (2003), E.I.T. Standard 1018-46, Wind Loading Code for Building Design (in Thai).
4. National Building Code of Canada (1995) issued by the Canadian Commission on Building and Fire Codes, National Research Council of Canada, Ottawa, Canada.
5. Boonyapinyo, V., Lukkunaprasit, P., Chucheepsakul, S., Warnitchai, P., Poovarodom, N., Thepmongkorn, S., Limsamphancharoen, N., and Leelataviwat, S. (2007), Wind Loading for Building Design in Thailand, Final Report, Thammasat University Research and Consultancy Institute (TU-RAC), Submitted to Department of Public Works and Town & Country Planning (in Thai); and DPT Standard (2007), DPT 1311-50: Wind Loading Calculation and Response of Buildings, Department of Public Works and Town & Country Planning (in Thai).
6. Boonyapinyo, V., Kritrachatanunt, A., and Janesupasaeree, K. (2005), Wind Load Comparisons among Several Codes with Wind Tunnel Experiment Data: Part 1 Comparisons of Calculation Method, Research and Development Journal of the Engineering Institute of Thailand, Vol.16, No.1, pp.1-14 (in Thai).
7. Boonyapinyo, V., Kritrachatanunt, A., and Janesupasaeree, K. (2005), Wind Load comparisons among several codes with Wind Tunnel Experiment Data: Part 2 Comparisons of Numerical Examples, Research and Development Journal of the Engineering Institute of Thailand, Vol.16, No.2, pp.15-24 (in Thai).
8. National Building Code of Canada (2005) issued by the Canadian Commission on Building and Fire Codes, National Research Council of Canada, Ottawa, Canada.
9. International Standard, ISO 4354 (1997) – Wind Actions on Structures, International Organization for Standardization, Switzerland.
10. ASCE Standard (2005), ASCE7-05: Minimum Design Loads for Buildings and Other Structures, American Society of Civil Engineers, New York.
11. AIJ (1996), Recommendation for Loads on Buildings, Architectural Institute of Japan.
12. Australian Standard, Minimum Design Loads on Structures (1989): Part 2 Wind Loads, Standards Australia, Sydney.
13. European Prestandard (1995), Ratified European Text, Eurocode 1: Basis of Design and actions on structures-Part2-4: Actions on Structures-Wind Actions. European Committee for standardization.
14. Mikitiuk, M., Surry, D., Lukkunaprasit, P., and Euasiriwan, N. (1995), Probability Based Wind Loadings for the Design of Transmission Structures, Part A-A Study of The Wind Climate for Thailand, Joint Research Report by Boundary Layer Wind Tunnel Laboratory, University of West Ontario and Chulalongkorn University, Thailand, CU/CE/EVR 1995.001.
15. Limsamphancharoen, N., Warnitchai, P., Boonyapinyo, V., and Poovarodom, N. (2007), Reference Wind Speed for Building Design in Thailand, Proc. of 12th National Convention on Civil Engineering, Pitsanuklok, Thailand, paper no. STR-097. (in Thai).

16. Poovarodom, N., Warnitchai, P., Petcharoen, C., Yinghan, P. and Jantasod, M. (2004), Dynamic Characteristics of Non-Seismically Designed Reinforced Concrete Buildings with Soft Soil Condition in Bangkok, Proc. of the 13th World Conference on Earthquake Engineering, Vancouver BC, Canada. Paper No. 1264, Oxford: Pergamon.
17. Plante, R.J. and Guard, C.P.(1990), 1989 Annual Tropical Cyclone Report, U.S. Naval Oceanography Command Center, Joint Typhoon Warning Center.
18. AIJ (2004), Recommendation for Loads on Buildings, Architectural Institute of Japan.
19. Boonyapinyo, V., Taleongpong, S., Sharma S. B., Periroek, A., and Thientim N. (2009), Wind Loads Study for MahaNakhon Building by Wind Tunnel Test : Part 1 Overall Wind Load Study and Part 2 Pressure Measurement Study, Final Report, Thammasat University Research and Consultancy Institute (TU-RAC), Submitted to Pace Development Co. Ltd.
20. Boonyapinyo, V., Warnitchai, P., Anwar, N., and Thientim N. (2009), Wind Tunnel Testing Study of Gramercy Building and Knighrbridge Building: Part 1 Pressure Measurement Study of Gramercy Building and Part 2 Pressure Measurement Study of Knighrbridge Building, Final Report, Thammasat University Research and Consultancy Institute (TU-RAC), Submitted to Century Properties, Inc.
21. ISO 10137 (1992), International Organization for Standardization, Bases for Design of Structures – Serviceability of Building against Vibration, Geneva.
22. Boonyapinyo, V., and Thamasungkeeti, W., (2010), Wind Load Study for Ramada Bangkok Sukhumvit Project by Wind Tunnel Test, Final Report, Thammasat University Research and Consultancy Institute (TU-RAC), Submitted to PBL Group and Rapos (Thailand) Co., Ltd.
23. Boonyapinyo, V., Janesupasaeree, T., and Thamasungkeeti, W. (2009), Identification of Flutter Derivatives of Bridge Decks by Stochastic Subspace Method, Proc. of 7th Asia-Pacific Conference on Wind Engineering, Taipei, Taiwan.
24. Boonyapinyo, V., and Janesupasaeree, T., (in print 2010), Data-Driven Stochastic Subspace Identification of Flutter Derivatives of Bridge Decks, *J. Wind. Eng. Ind. Aerodyn.*, 16 p.
25. Sarkar P.P., Jones N., and Scanlan R.H. (1994), Identification of Aeroelastic Parameters of Flexible Bridges, *J. Eng. Mech., ASCE* , 120 (8), 1718–1741
26. Jakobsen J.B., and Hjorth-Hansen E. (1998), Aeroelastic Effects on a Rectangular Box-Girder Bridge, *J. Wind. Eng. Ind. Aerodyn.*, 74-76, 819–827.
27. Gu M., and Qin X.R. (2004), Direct Identification of Flutter Derivatives and Aerodynamic Admittances of Bridge Decks, *Eng. Struct*, 26, 2161–2172.
28. Boonyapinyo V., Miyata, T. and Yamada, H. (1999), Advanced Aerodynamic Analysis of Suspension Bridges by State-Space Approach, *J. Struct. Eng, ASCE*, 125(12), 1357-1366.